The Effect of Geometry on Contact Conductance of Contiguous Interfaces

B. J. Rozon,* P. F. Galpin,* G. E. Schneider,† and M. M. Yovanovich‡
University of Waterloo, Waterloo, Ontario, Canada

An analysis to determine the thermal resistance across contiguous, rough interfaces is presented. Numerical solutions using the finite element method are presented for a range of the governing geometric and thermal parameters and for three interfacial configurations. The three interface shapes examined are the saw-tooth, sine-wave, and square-wave profiles. It is observed that in all cases the influence of the interface presence is to decrease the resistance below the one-dimensional, smooth-interface value. This observation is supported through application of Elrod's two theorems to the problem configuration. Numerical solutions for the decrease in resistance, estimated to be within 1% of their true values, are presented for a range of conductivity ratios and interface amplitudes. It was observed that the effect of increasing both of these parameters is to decrease the resistance due to the presence of the interface.

Nomenclature

A	= amplitude of interface profile
B	= thickness of analysis section
H	= length of analysis section
k	= conductivity
n	= normal to interface
R	= resistance
δR	= incremental resistance, $= R_{1\text{-}D} - R_{TOT}$
T	= temperature
W	= width of analysis section
x,y	= Cartesian coordinates

Superscript

$(\ )^*$	= nondimensional

Subscripts

i	= interface
TOT	= total
1-D	= one-dimensional
1,2	= material identifiers

Introduction

MANY engineering applications encounter interfaces in which, although intimate contiguous contact may exist, the cross section of the interface is such that the thermal field is locally highly two- or three-dimensional in the vicinity of the interface. Examples of such contiguous interfaces are those that result from electroplating of a rough surface, explosion bonding of two dissimilar materials, and the penetration of the large asperities of a very rough, hard substrate into a thick but, relatively much softer, intermediate material. The object of such applications is to reduce the thermal interfacial resistance to heat transfer, with modern computing equipment finding great application of these devices as the local power density continues to increase.

In modern mainframe computers, a typical heat sink to remove thermal energy from high-density electrical traffic areas consists of a water-cooled, cold plate mechanically attached to the microelectronics housing. As computers increase in size, and therefore the required cold-plate surfaces also increase in size, it becomes difficult, if at all possible, to

manufacture flat surfaces of the required dimensions. When a surface possesses waviness in addition to roughness, the actual contact area consists of discrete contact spots that form in clusters within certain portions of the contact plane. The heat transfer across such interfaces occurs through the contact spots and by conduction through the interstitial (usually atmospheric air) fluid. This thermal resistance is both significant and uncontrollable.

Several methods have been proposed to reduce and control this important interfacial resistance. One proposed method consists of a smooth, thick layer of a soft material bonded to the surface of the microelectronics housing. The cold-plate surface is machined to produce a very rough surface, with such roughness being in excess of the inherent waviness. This then ensures intimate contact over the entire interface when the rough cold plate is bolted against the softer layer. Both saw-tooth and square-wave profiles have been proposed for this purpose. Other methods include electroplating, explosion bonding, and soldering or brazing. In these cases the microcontact resistance at the interface will not affect the results of this paper. In the bolted case, this microcontact resistance will alter the absolute value of the resistances quoted herein, but will not influence the trends of resistance reduction presented.

Although limited experimental data have been provided for explosive bonded interfaces,[1] the problem of determining the thermal resistance across contiguous, rough interfaces has not yet been successfully analyzed from a theoretical viewpoint. It is the purpose of this paper to examine this problem and, in particular, to determine the influence of interfacial geometry and mating material conductivities on the thermal resistance of contiguous, rough interfaces. Three specific interfacial geometries will be examined in a two-dimensional formulation.

Mathematical Formulation of the Problem

A typical section of a contiguous rough interface is illustrated in Fig. 1. The shape of the interface as shown is strongly representative of a sinusoidal interface, while the other configurations considered here are saw-tooth and square-wave interfaces. Under the quite reasonable assumption that the dimensions of the roughness are small relative to the breadth of the contacting members and that the heat-flow environment at the energy addition and rejection surfaces is uniform across the breadth, at least locally, the cell shown by the dashed rectangle in Fig. 1 can be extracted as a typical analysis geometry.

The typical analysis cell is shown in Fig. 2 where the lateral boundaries at $x = 0$ and W are assigned adiabatic boundary
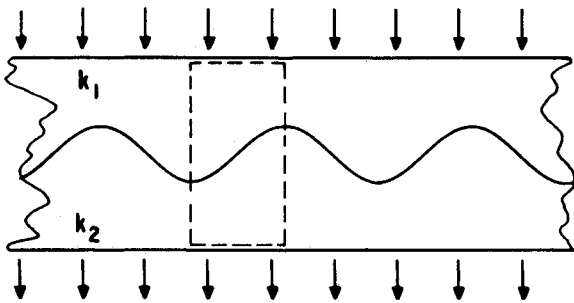
Fig. 1 Problem geometry.

conditions to reflect the symmetry about these surfaces in the original geometry of Fig. 1. The interface shape is denoted by $y_i(x)$ in the figure and can represent a sinusoidal shape, a saw-tooth profile, or a square-wave configuration. The boundary conditions at the top and bottom surfaces are specified Dirichlet conditions at different temperatures, and for sufficiently large H/W, as will be seen, this specification is consistent with a uniform flux over these surfaces.

With reference to Fig. 2, the following nondimensional variables are introduced.

$$T^* \equiv \frac{T - T_2}{T_1 - T_2} \qquad (1)$$

$$x^* \equiv x/W, \qquad y^* \equiv y/W \qquad (2)$$

$$k^* \equiv k/k_1 \qquad (3)$$

The mathematical problem can then be formulated as follows:

$$\frac{\partial^2 T_j^*}{\partial x^{*2}} + \frac{\partial^2 T_j^*}{\partial y^{*2}} = 0, \qquad j = 1,2 \qquad (4)$$

where $j = 1$ denotes the region above the interface and $j = 2$ denotes the region below the interface. The boundary conditions are given by

$$\frac{\partial T_j^*}{\partial x^*}(0, y^*) = 0 \qquad (5a)$$

$$\frac{\partial T_j^*}{\partial x^*}(1, y^*) = 0 \qquad (5b)$$

$$T_2^*(x^*, -H/2W) = 0 \qquad (5c)$$

$$T_1^*(x^*, H/2W) = 1 \qquad (5d)$$

The compatibility conditions existing at the interface are

$$T_1^*(y^* = y_i^*(x^*)) = T_2^*(y^* = y_i^*(x^*)) \qquad (6a)$$

and

$$-\frac{\partial T_1^*}{\partial n^*}\bigg|_{y^* = y_i^*(x^*)} = -k_2^* \frac{\partial T_2^*}{\partial n^*}\bigg|_{y^* = y_i^*(x^*)} \qquad (6b)$$

where n^* is a nondimensional coordinate normal to the interface directed from material 1 into material 2. Further, the interface is located symmetrically about the line $y^* = 0$.

The total thermal resistance for the typical analysis cell is defined by

$$R_{TOT} = \frac{[T_1 z - T_2]}{\int_0^W k_1 \frac{\partial T_1}{\partial y}\bigg|_{y = H/2} B dx} \qquad (7)$$
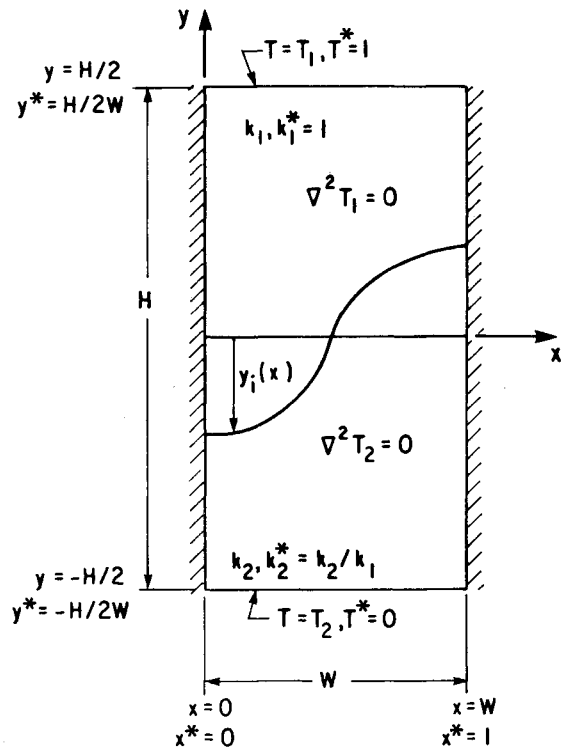

Fig. 2 Typical analysis cell.

where B is the extent of the analysis cell perpendicular to the cross section shown in Fig. 2. A nondimensional resistance can be defined as

$$R_{TOT}^* \equiv R_{TOT} k_1 B = \left[\int_0^1 \frac{\partial T_1^*}{\partial y^*}\bigg|_{y^* = H/2W} dx^* \right]^{-1} \qquad (8)$$

Since the temperature field has the functional dependence given by

$$T^* = T^*(x^*, y^*, H/W, k_2^*, A^*, \text{shape}) \qquad (9)$$

it follows that the nondimensional resistance has the functional dependence

$$R_{TOT}^* = R_{TOT}^*(H/W, k_2^*, A^*, \text{shape}) \qquad (10)$$

where A^* denotes the nondimensional amplitude of the interfacial profile measured from the centerline, $y^* = 0$, and "shape" denotes the geometric configuration of the interface, i.e., sinusoidal, saw-tooth, square-wave.

The preceding nondimensional resistance has, as an intrinsic component, the bulk resistance of the material distant from the interface where the thermal field is uniform. This component is manifested by a continuous increase in R^* as H/W increases, when, in fact, the influence of the interface itself rapidly approaches an asymptotic limit as H/W increases. To remove this direct dependence on H/W, for sufficiently large H/W, the incremental resistance is defined according to

$$\delta R^* \equiv R_{1\text{-}D}^* - R_{TOT}^* \qquad (11)$$

where

$$R_{1\text{-}D}^* = \frac{H}{2W}\left[1 + \frac{1}{k_2^*}\right] \qquad (12)$$

represents the one-dimensional resistance that would exist if the interface existed as a perfectly smooth, but contiguous,

surface located at $y^* = 0$. The reasons for defining δR^* according to Eq. (11) rather than as its negative will become more apparent when the results are presented.

Using the preceding definition for δR^*, its functional form can be represented as

$$\delta R^* = \delta R^*(H/W, k_2^*, A^*, \text{shape}) \qquad (13)$$

Further, considering large H/W, it can be demonstrated that, to within less than 0.5%, the incremental resistance is invariant with H/W for values of $H/W > 3$ provided that the amplitude of the interface is less than $W/2$, or nondimensionally if $A^* \leq 0.5$. Since these conditions are highly representative of those most frequently encountered in practice, we have the functional dependence

$$\delta R^* = \delta R^*(k_2^*, A^*, \text{shape}); \qquad (H/W) > 3, A^* < \frac{1}{2} \qquad (14)$$

which exhibits the primary dependencies of interest in this work. These are the dependencies of the incremental resistance on the materials combination, on the amplitude of the interface, and on the geometric configuration of the interface itself. The three specific geometric profiles examined are: 1) saw-tooth, 2) sinusoidal, and 3) square-wave.

Numerical Solution

The governing partial differential equations, together with boundary conditions, were solved numerically using the finite element method.[2] The nine-noded, isoparametric, quadratic, quadrilateral finite element was employed[3] and a Galerkin formulation of the finite element equations was used. Details regarding the element and the equation formulation can be found in Refs. 3 and 4. Having determined the temperature field using the finite element procedure, the heat flows were determined through postprocessing of the resulting data and, consequently, both the total and incremental resistances could be determined.

Typical meshes used in the discretization are shown in Fig. 3 for the three interface configurations examined. In this figure, the intersection of the indicated grid lines identifies the nodal locations employed throughout the domain, and, although the plotting was performed using a piecewise linear interpolation between nodal locations, the actual elemental configuration conforms to the isoparametric, quadratic, quadrilateral element. The meshes shown in the figure correspond to H/W values of 3 for all three interface configurations and are representative of the actual discretization employed in obtaining the data presented herein. Note that several alternative mesh-generation algorithms were examined and the numerical

results obtained using these alternative meshes support the results obtained using the meshes indicated.

To support the previous assertion that the incremental resistance becomes independent of H/W for values of H/W in excess of 3, a study was conducted to examine this dependence. The results of this study, for the extreme case of $A^* = \frac{1}{2}$ and $k_2^* = 100$, are shown in Fig. 4. In this figure it is seen that as H/W exceeds 3, the value of δR^* indeed becomes independent of further increases in H/W. The major dependence of δR^* on H/W occurs only for very small values of H/W, and at these smaller values of H/W the exhibited variation is a reflection of the extreme thermal stiffness of the problem due to the close proximity of the Dirichlet boundaries to the actual interface. In practice, this is a further reflection of the difficulty that would be experienced in maintaining the boundaries in an isothermal condition for such configurations.

Convergence studies were also conducted to ascertain the mesh refinement level necessary to achieve satisfactory results. The results of these studies are presented in Figs. 5 and 6 for the extreme combination of $A^* = \frac{1}{2}$ and $k_2^* = 100$. Figure 5 presents the convergence study results for the three interfacial configurations in terms of the total resistance. It is clear that the convergence of the total resistance is rapid and asymptotic. Two levels of discretization were used and correspond to 80, 80, and 84 elements for the saw-tooth, sine-wave, and square-wave cases, respectively, providing results estimated to be within 0.1% of the converged, mesh-independent asymptotes. Since the incremental resistance is of direct interest in this work, however, the mesh-dependent characteristics of the incremental resistance were also examined. These are presented in Fig. 6. Again, convergence is rapid and asymptotic. The scale of the ordinate in these curves is highly expanded, and it is estimated that for 80, 80, and 84 elements for the saw-tooth, sine-wave, and square-wave configurations, respectively, the error in the incremental resistance is less than 1%. It is noted that the convergence studies were performed for configurations in which the two-dimensionality of the thermal flowfield is highest and, therefore, the accuracy of other configurations is expected to be higher than that previously quoted. Therefore it is estimated that the accuracy of all values of the incremental resistance presented herein will be within 1%.
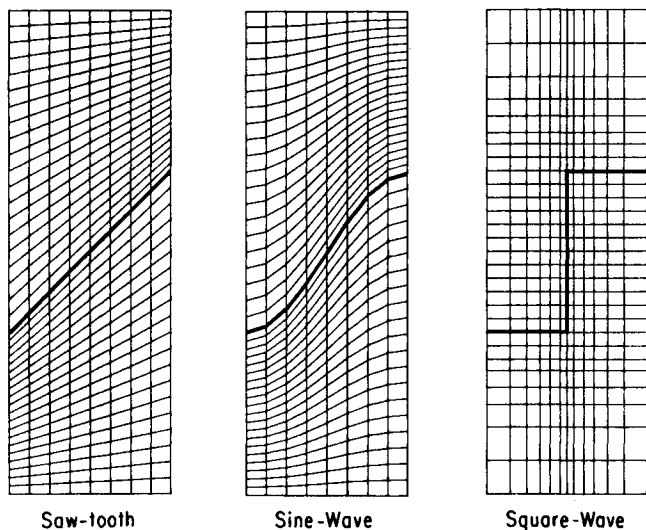

Saw-tooth   Sine-Wave   Square-Wave

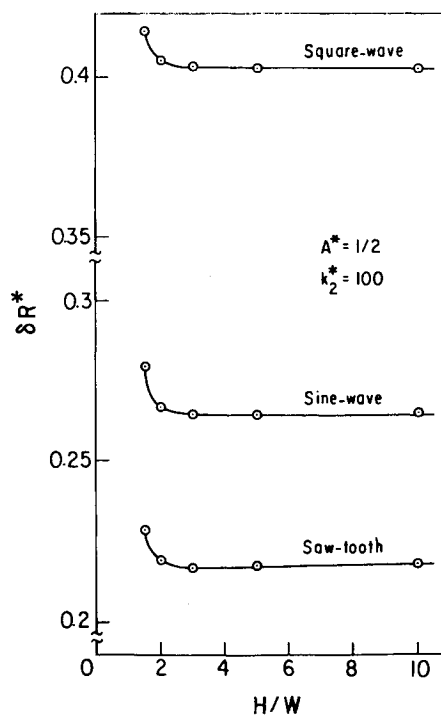Fig. 3   Discrete finite element meshes employed.
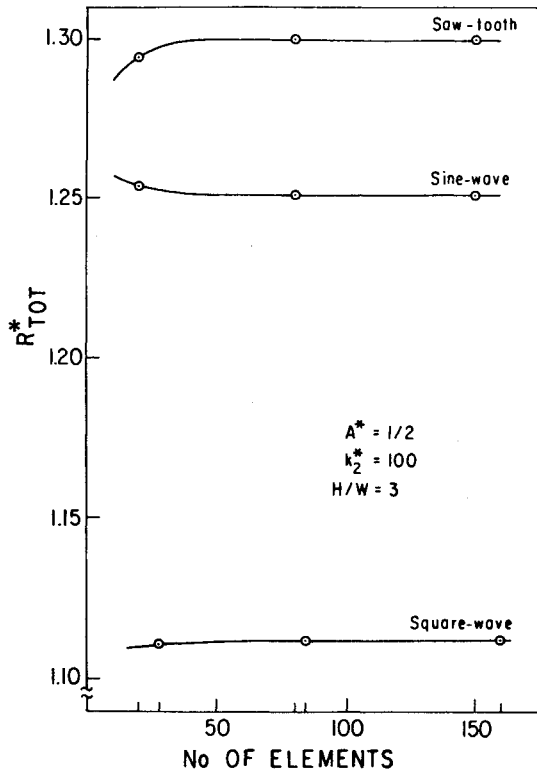

Fig. 4   Dependence of δR^* on H/W.
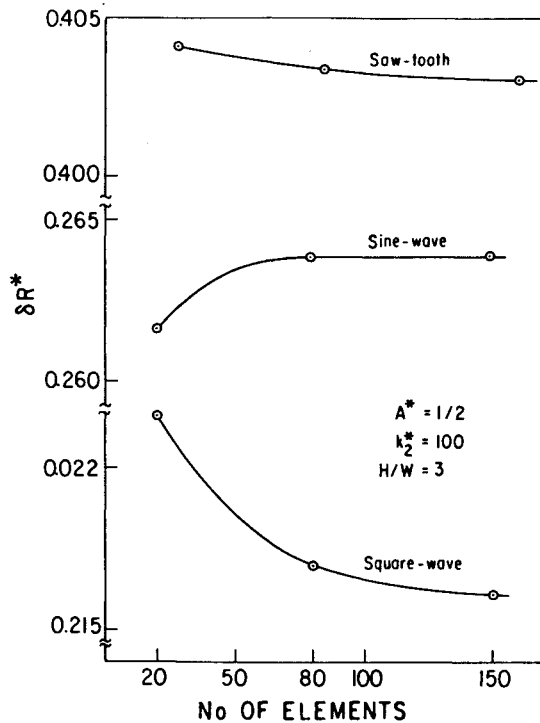
Fig. 5   Convergence study for R^*_{TOT}.

Fig. 6   Convergence study for δR^*.

Results

In this section numerical results are presented for the three interfacial configurations for a wide range of interfacial amplitudes and material conductivity ratios. All results are presented for $H/W = 3$, which was previously shown to be highly representative of the incremental resistance. Typical contour plots of the isotherms for this H/W, $A^* = \frac{1}{2}$, and $k^*_2 = 100$ are presented in Fig. 7. These contour plots further support the H/W conclusions previously advanced since it is clear from these figures that the disturbance exhibited in the
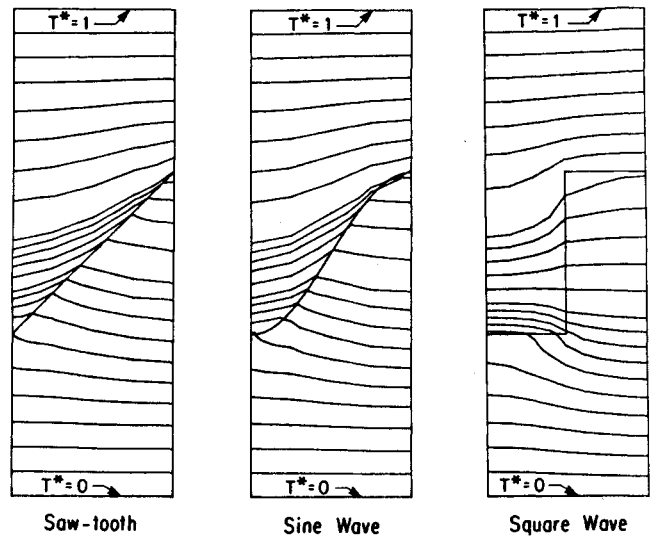

Fig. 7   Contour plots of temperature for $H/W = 3$, $k^*_2 = 100$, $A^* = \frac{1}{2}$.

vicinity of the interface has not propagated to the endface regions of the domain and the thermal field in these end regions is indeed highly regular and one-dimensional.

Further, the incremental resistance, as defined earlier, is positive in all cases examined as shown in Figs. 8-10. This positive nature of the incremental resistance means that the presence of the interface results in a *decrease* in resistance from that experienced in the one-dimensional case. It had been previously suggested that the distortion of the thermal field due to the presence of the interface would result in an increase in the thermal resistance.[1] However, the present results indicate conclusively and quantitatively that the overall resistance is decreased due to the presence of the interface, when compared to the perfectly flat interface configuration, and, in addition, that this decrease in resistance can be appreciable.

Figure 8 presents the incremental resistance for the saw-tooth interfacial configuration. It is seen from this figure that the influence of increasing both the interfacial amplitude and the conductivity ratio is to increase the incremental resistance and, therefore, to decrease the total resistance. The trends in the figure indicate that small interface amplitudes lead to relatively small decreases in total resistance. As the interface amplitude increases, however, the decrease in resistance grows rapidly. Results are presented for conductivity ratios of 5, 10, and 100, which encompass the range of greatest practical utility. At large conductivity ratios, the influence of further increasing the conductivity ratio diminishes in its effect on the incremental resistance. This is evidenced by comparing the change in incremental resistance which results from doubling this ratio from 5 to 10 vs the order-of-magnitude change that results from a change in conductivity ratio from 10 to 100. For both of these latter cases the changes in incremental resistance are comparable.
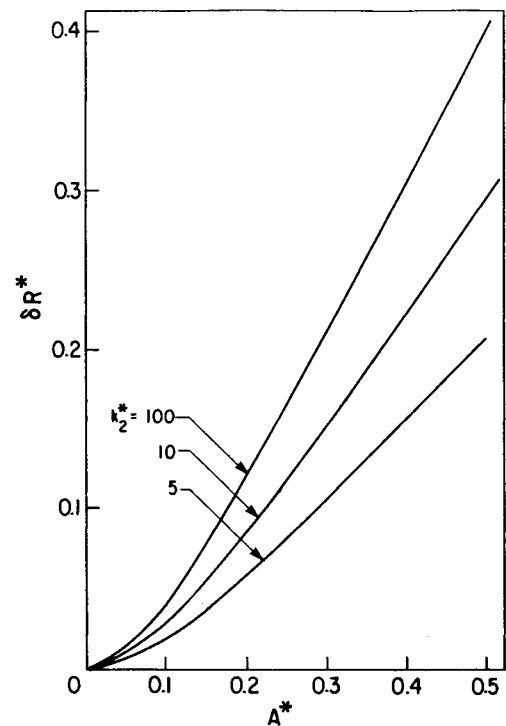
Figures 9 and 10 present the incremental resistance results for the sine- and square-wave interfacial configurations, respectively. It is observed that, although the actual numerical data is different for all three configurations, the trends displayed by the data of Figs. 9 and 10 are exactly analogous to those discussed above for the saw-tooth configuration. As such, these results do not require further explanation. It is observed, however, that there is a geometric hierarchical structure displayed by Figs. 8-10. For all values of A^* and k^*_2, the reduction in resistance, i.e., the magnitude of δR^*, is smallest for the saw-tooth configuration, while the sine-wave results fall intermediate between the saw-tooth and square-wave results for all values of A^* and k^*_2. This is a direct result of the increasing volumetric penetration of higher conductivity material into the lower conductivity region as the sequence is

Fig. 8 Saw-tooth δR^* results.
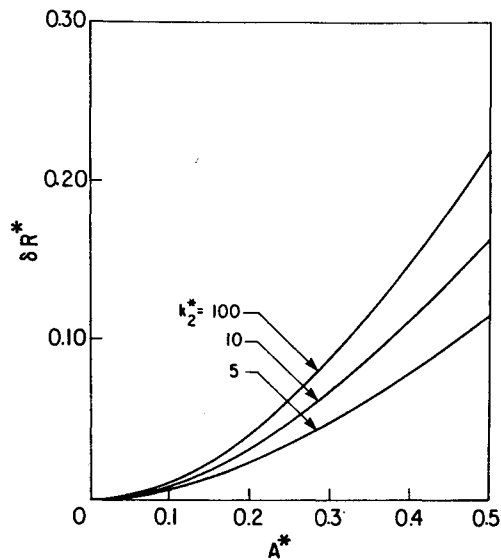
Fig. 9 Sine-wave δR^* results.
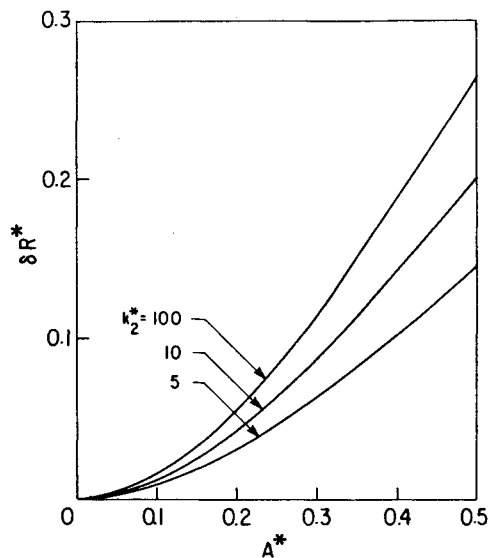
Fig. 10 Square-wave δR^* results.

progressed from saw-tooth to sine-wave to square-wave configuration. Based on this line of reasoning, it can therefore be argued that the greatest incremental resistance possible, i.e., the greatest reduction in resistance, will be that of the square-wave geometry if groove/interface shapes of the re-entrant configuration are excluded.

The further observation can be made in Fig. 10 that for amplitudes A^* greater than approximately $A^* = 0.2$, the incremental resistance for the square-wave configuration increases linearly with nondimensional amplitude. This is believed to be due to the significant portion of the interface profile that is parallel to the sidewalls in the central region of the analysis cell. While there is a significant distortion of the thermal field in the vicinity of the peak and trough of the square-wave interface, the effect of a continued increase in the amplitude of the square-wave interface is to add a section of material in which the thermal field is relatively undistorted and for which the apparent conductivity corresponds to that of high- and low-conductivity material in parallel. This modified (and higher than unity) conductivity displaces the unity conductivity inherent in the one-dimensional configuration.

In demonstration of this, the curve corresponding to $k_2^* = 100$ in Fig. 10 can be examined. For this case, in the one-

dimensional model the resistance is almost exclusively due to the low-conductivity material. Conversely, in the square-wave central region, the apparent parallel conductivity relative to the base material approaches zero. The rate of reduction of resistance with the increasing A^* is then directly proportional to the rate of replacement of base material having unity conductivity with the parallel composite having infinite conductivity in the limit of very large k_2^*. This is lucidly demonstrated by the $k_2^* = 100$ curve of Fig. 10 which exhibits a slope remarkably close to unity, i.e., the $k_2^* \to \infty$ limiting value.

The fact that the interface presence results in a decrease in total resistance, i.e., a positive incremental resistance, can be further demonstrated through application of the theorems presented by Elrod.[5] These theorems have been successfully employed in the past[6] to provide very economical, accurate estimates for the thermal resistance of engineering systems. Unfortunately, their utility is not as great in the present work as evidenced by the large difference between the upper and lower bounds shown in Fig. 11 for $k_2^* = 100$ and the saw-tooth profile. The upper and lower curves of this figure correspond to the upper and lower incremental resistance, as determined using Elrod's theorems, with the actual numerically determined values shown as the intermediate curve. While the bounds cannot be used to quantify the incremental resistance accurately, they do undeniably demonstrate that the influence of the interface is to reduce the system resistance providing positive values for δR^*. Results similar to those shown in Fig. 11 were obtained for the remaining conductivity ratios and for the other interface shapes.

Finally, as a demonstration of the impact that the resistance reduction can have on system resistance, the curves in Fig. 12 are presented. This figure presents, for the saw-tooth interface and $A^* = \frac{1}{2}$, the reduction in resistance divided by the one-dimensional resistance. Clearly, as H/W increases to large values along the abscissa, the impact of the interface becomes less important, as shown. However, as shorter lengths are considered, the impact of the interfacial resistance reduction increases dramatically. For $k_2^* = 100$, for example, and at $H/W = 2$, the reduction in resistance due to the interface is 30% of the one-dimensional value! This is clearly a significant reduction. It is noted that in the construction of Fig. 12, for
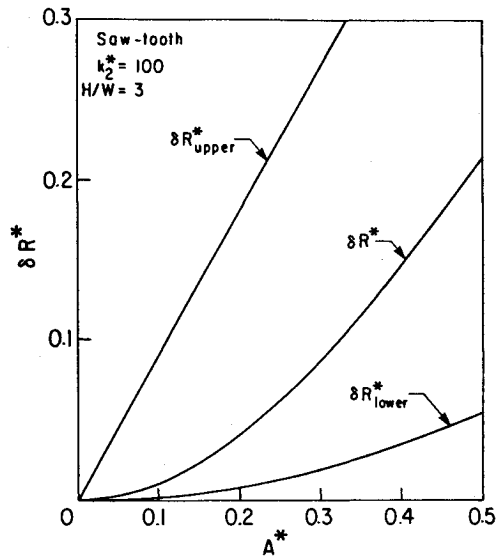
Fig. 11   Typical comparison of δR^* with upper and lower bounds prediction.
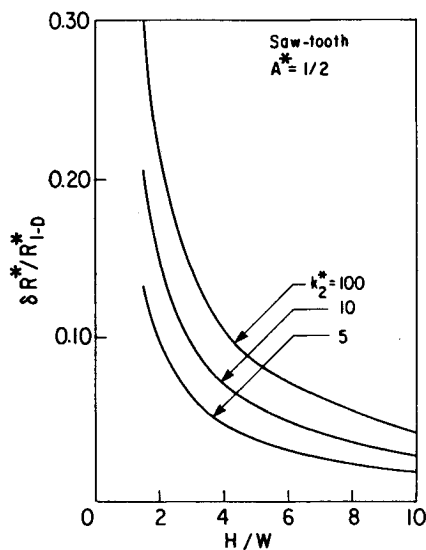

Fig. 12   Relative importance of δR^* vs H/W for saw-tooth profile $A^* = \frac{1}{2}$.

$H/W < 3$, the actual values of δR^* have been employed. Clearly, where the parent materials (or coating, perhaps) are relatively thin, there is a significant resistance reduction available through the use of rough, contiguous interfacial profiles. As miniaturization within the microelectronics industry continues, situations in which the resistance reduction is appreciable are becoming more and more typical.

Discussion and Conclusions

The problem of determining the resistance to heat flow across two-dimensional contiguous, rough interfaces has been addressed in this work. Three specific interfacial configurations have been explicity considered: the saw-tooth, sine-wave, and square-wave interfaces. Steady-state conditions were examined and numerical solutions were obtained using the finite element method with the nine-noded, isoparametric, quadratic, quadrilateral elments employed for all solutions. It was shown that for $H/W > 3$, the incremental resistance, the departure from the one-dimensional, flat interface configuration, is independent of further increases in H/W. Subsequently, the parametric studies were conducted for $H/W = 3$.

The results of the parametric studies indicate that in all cases the influence of the interface profile is to decrease the resistance of the system below the one-dimensional evaluation. While it had been previously suggested that the heat flow field distortion resulting from the presence of the interface would lead to higher resistances than those obtained in the one-dimensional configuration, the results presented here indicate that the resistance, without exception, is decreased due to the presence of the interface profile. This conclusion has been further supported by application of the theorems of Elrod. In this analysis both the upper and lower bounds on the resistance indicate that a decrease in resistance from the one-dimensional case will result when contiguous, rough interfaces are employed.

The present study is the first study to quantify the change in resistance for such configurations. Based on convergence studies, it is estimated that the solutions presented are within 1% of the actual value of the incremental resistance. For the three interface configurations, results have been presented for a range of conductivity ratios, k_2^*, and for a range of interface amplitudes, A^*. The effect of both parameters is that increasing their value also increases the reduction in the resistance. Futher, a hierarchy of interface shapes emerged. It was observed that the reduction in resistance increases as the amount of material displayed by the interface increases. Thus the saw-tooth profile led to the least reduction in resistance, while the square-wave profile led to the highest reduction in resistance. It is expected that these results will be of value in the design of thermal systems, and in particular to the design of interfacial systems associated with the heat-removal systems of compact, high-density, microelectronic components.

References

[1]Yovanovich, M.M., Cecco, V. S., and Schneider, G. E., "Electrical Constriction Resistance and Potential Field Mapping of Explosive Bonded Interfaces," AIAA Paper 80-0088, Jan. 1980.

[2]Schneider, G. E., "Finite Elment Formulation of the Heat Conduction Equation in General Orthogonal Curvilinear Coordinates," *ASME Journal of Heat Transfer,* Vol. 98, Ser. C, Aug. 1976, pp. 525-527.

[3]Raw, M. J., Hassani, V., and Schneider, G. E., "Development and Evaluation of Nine-Noded Quadratic Control Volume Based Finite Element for Heat Conduction Modelling," *Journal of Spacecraft and Rockets,* Vol. 22, Sept.-Oct. 1985, pp. 523-529.

[4]Huebner, K. H., *The Finite Element Method for Engineers,* John Wiley & Sons, New York, 1975.

[5]Elrod, H. G., "Two Simple Theorems for Establishing Bounds on the Total Heat Flow in Steady-State Heat Conduction Problems with Convective Boundary Conditions," *Journal of Heat Transfer,* Vol. 96, Ser. C, 1974, pp. 65-70.

[6]Yovanovich, M. M., Schneider, G. E., and Strong, A. B., "Transverse Apparent Thermal Conductivity of Long Rectangular Fibers in a Matrix," ASME Paper 75-HT-26, Aug. 1975.